Journal of Hazardous Materials 164 (2009) 683–688

Contents lists available at ScienceDirect

Journal of Hazardous Materials

journal homepage: www.elsevier.com/locate/jhazmat

The role of weathering on fly ash charge distribution during triboelectrostatic beneficiation

Federico Cangialosi[a,*], Michele Notarnicola[a], Lorenzo Liberti[a], John Stencel[b]

[a] Department of Environmental Engineering and Sustainable Development, Technical University of Bari, viale del Turismo 8, 74100 Taranto, Italy
[b] Tribo Flow Separations, Lexington 40511, KY, USA

ARTICLE INFO

Article history:
Received 18 October 2007
Received in revised form 18 August 2008
Accepted 18 August 2008
Available online 23 August 2008

Keywords:
Triboelectrostatic separation
Weathering
Fly ash
Particle charge distribution

ABSTRACT

Triboelectrostatic beneficiation of coal combustion fly ashes with high-unburned carbon contents can produce low-carbon ash products having value as mineral admixtures and meeting technical requirements for replacing cement in concrete. This capability is a result of establishing bipolar charge on mineral ash versus carbon particles where, typically, unburned carbon attains positive surface charge and ash attains negative surface charge under the tribocharging conditions employed in triboelectrostatic technologies. However, long-term exposure of fly ash to weathering conditions, such as moisture or high humidity, before beneficiation is known to dramatically diminish carbon–ash separation efficiencies. Although experimentation has shown that water soluble surface species can be redistributed on fly ash particles after exposure to moisture, which could affect the extent of charging and polarities, measurement of the actual amount of charge and polarity on particles after weathering exposure versus after removal of surface moisture has not been accomplished. Hence, a new experimental methodology was developed and applied to measure charge distributions on tribocharged ash and carbon particles in a fly ash that had been exposed to weathering conditions for 6 months before and after removal of the surface moisture. Weathered ash particles were found to have an average zero charge, whereas carbon particles attained an average negative charge, opposite of the normal polarity for carbon. Although the extent of uncharged particles decreased and ash particles attained an average negative charge after drying, carbon particles attained only an average zero charge. These changes were reflected in very small increases in carbon–ash separation efficiency, in contrast to previous beneficiation tests in which fly ash drying led to significant increases in carbon–ash separation efficiency. It is suggested that removal of surface moisture in the absence of other processes like surface ion redistribution would beneficially impact carbon–ash triboelectrostatic beneficiation.

1. Introduction

Triboelectrostatic beneficiation has been investigated by several researchers [1–4] as a method to separate physically distinct particles on the basis of electronic surface properties as characterized by material work functions. These studies relate to triboelectrostatic technologies that have been commercialised for fly ash beneficiation [2,5] in which carbon-enriched particles are physically separated from ash-enriched particles to meet requirements for fly ash use as a valuable mineral admixture replacing cement in concrete mixtures. Independent of the technology, bipolar particle charging is established by particle–particle or particle–container collisions under turbulent flow, after which it is possible to separate carbon and ash particles within an electric field. It is generally observed that the establishment of charge, called tribocharging, on fly ash produces positively charged carbon and negatively charged ash particles [6].

Several factors influence the physical and chemical surface properties of carbon and ash particles that also cause variation in their tribocharging properties. Water adsorption, for example, caused a majority of carbon particles to report to the positive electrode product during beneficiation, i.e. were negatively charged, and a decrease in carbon–ash separation efficiency [7]; these beneficiation changes were related to changes in soluble surface ion concentrations. Although the effects of surface moisture on the triboelectrostatic beneficiation of ashes could be mostly reversed by drying of the ashes [8], the effects of moisture on particle charge and polarity was not measured. In particular, it is not known how moisture adsorption during ash weathering affects the mineral ash and unburned carbon from a charging behaviour standpoint, nor if the effects are always reversible with heat treatment. This study addresses these issues by introducing a methodology to evaluate

* Corresponding author. Tel.: +39 099 4734243; fax: +39 099 4733304.
E-mail address: f.cangialosi@poliba.it (F. Cangialosi).

0304-3894/$ – see front matter © 2008 Elsevier B.V. All rights reserved.
doi:10.1016/j.jhazmat.2008.08.050

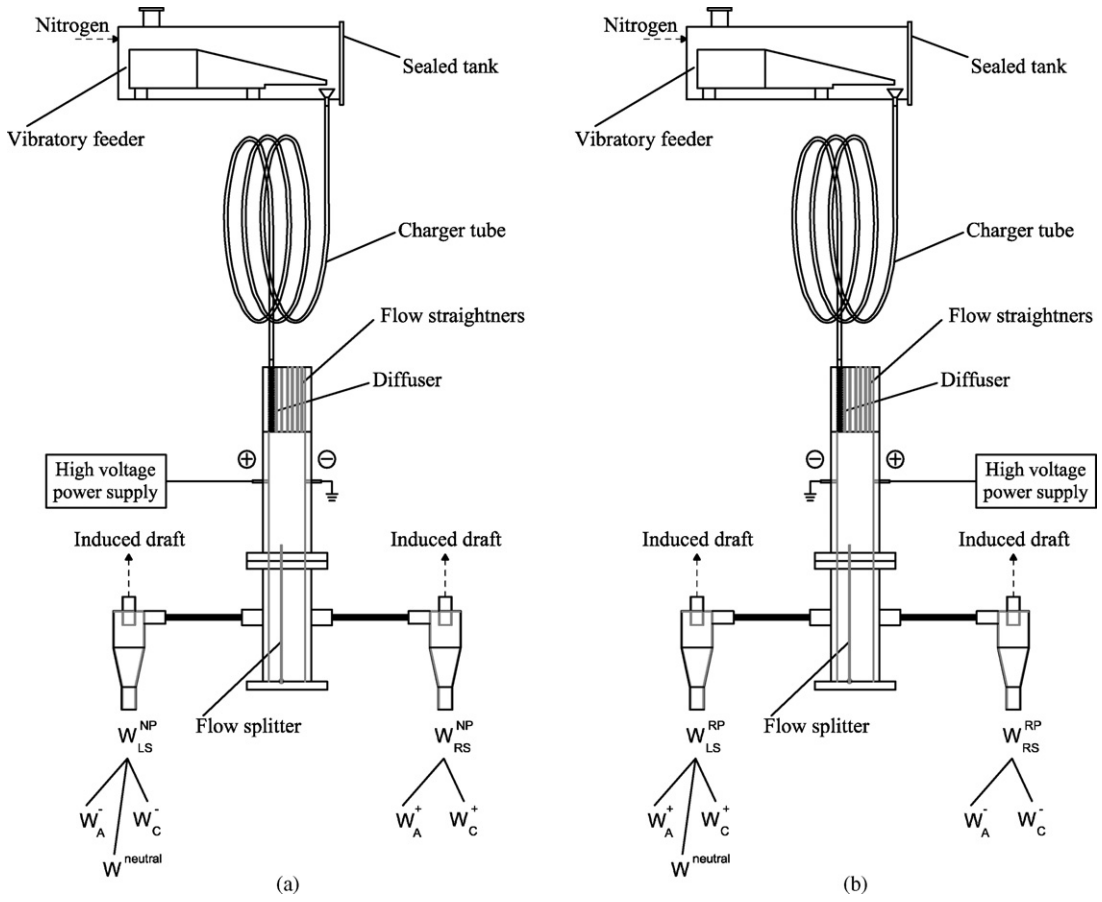

Fig. 1. Schematic configuration of bench scale triboelectrostatic separator in NP (a) and RP (b) operation modes.

the charge distribution on ash and carbon particles before and after drying of weathered fly ash samples.

2. Materials and methods

2.1. Sample treatments

The fly ash used in this study was from an Italian coal-fired power plant and had an average LOI (loss on ignition) of 30%. Charging and charge distribution studies were initiated 6 months after ash collection from the utility; in the intervening period no precautions were taken to limit exposure of the ash to environmental or atmospheric conditions. In other words, the ash experienced weathering due to effects of exposure to an uncontrolled atmosphere. The carbon–ash separation efficiency of this weathered ash (hereafter, weathered ash = W-ash) was compared to that of the ash immediately after collection (hereafter, freshly collected ash = FC-ash) and to that of the weathered ash dried at 105 °C for 24 h and placed in a sealed container before being processed (hereafter, weathered and dried ash = WD-ash). Because the procedure for measuring charge and polarity was developed long after collecting the ash, only the charge distribution on weathered and weathered-then-dried samples have been closely examined.

2.2. Experimental methodology

The methodology employed two experimental configurations to develop charge distribution curves for particles entering the triboelectrostatic separation chamber. In the first configuration (Fig. 1a), hereafter referred to as normal polarity (NP), particles were injected close to the positive electrode of the electric field cell (Tribo Flow Separations, Lexington, KY, USA) described elsewhere [8]. The voltage potential across the electrodes was varied between 0 and 12 kV. In this configuration neutral and negative particles were collected by the cyclone on the positive polarity side (left side in Fig. 1a), whereas only positive particles were deflected by the electric field and collected in the negative polarity side. The second configuration, hereafter referred to as reverse polarity (RP), particles were injected close to the negative electrode of the electric field cell so that only neutral and positive particles were collected by the cyclone on the negative side (left side in Fig. 1b), and only negative particles were collected by the cyclone of the positive polarity side (Fig. 1b). By using equal process conditions (electric field strength, gas velocity and feed rate) during operation under NP and RP configurations, it was possible to determine the mass fractions of positively and negatively charged particles (W_A^+, W_A^-, W_C^+, and W_C^-) as well as the amount of poorly charged (neutral) particles ($W_A^{neutral}$ and $W_C^{neutral}$) with the following material balance equations:

$$\begin{cases} W_{LS}^{NP} = W_A^- + W_C^- + W_A^{neutral} + W_C^{neutral} \\ W_{RS}^{NP} = W_A^+ + W_C^+ \\ W_{LS}^{RP} = W_A^+ + W_C^+ + W_A^{neutral} + W_C^{neutral} \\ W_{RS}^{RP} = W_A^- + W_C^- \\ W_C^- = W_{RS}^{RP} \cdot \mathrm{LOI}_{RS}^{RP} \\ W_C^+ = W_{RS}^{NP} \cdot \mathrm{LOI}_{RS}^{NP} \end{cases} \quad (1)$$

Table 1
Mass balance of tests in NP and RP configurations for W-ash (LOI = 30%)

Voltage (kV)	Ash mass (%)			Carbon mass (%)		
	Positive	Negative	Neutral	Positive	Negative	Neutral
0.0	6.0	6.2	87.8	2.6	3.0	94.4
3.0	18.0	11.9	70.1	4.0	8.3	87.6
6.0	32.4	21.3	46.3	10.2	18.3	71.6
9.0	41.9	26.7	31.4	24.8	34.8	40.5
12.0	48.7	35.9	15.5	38.0	47.1	14.9

Table 2
Values of critical charge associated with electric field voltages

Voltage (kV)	Particle charge (pC)	
	Ash	Carbon
3	0.005	0.25
6	0.0024	0.12
9	0.0016	0.085
12	0.0012	0.061

where: W_j^i is the mass collected on the jth side of the separator (left or right, according to Fig. 1) in the ith configuration using NP or RP; LOI_j^i is the loss on ignition collected in the jth side of the separator (left or right, according to Fig. 1) in the ith configuration (NP or RP).

The two test configurations were used for testing the weathered (W-ash) and weathered-then-dried ashes (WD-ash) at different voltages to estimate the percentage of particles moving under the influence of changing electric field forces. More particles with progressively lower charge were forced towards the electrode opposite of the injection point as the electric field intensities were increased. When high electric field intensities were used, even particles with very low charge were forced to move across the electric field cell. Those particles that did not move away from the collection zone immediately under the injector were considered neutral or very poorly charged. It was then possible to measure the incremental mass fractions of ash and carbon particles of both polarity (ΔW_A^+, ΔW_A^-, ΔW_C^+, and ΔW_C^-) moving when the electric field was changed from E to $E+\Delta E$. The corresponding charge needed to deflect the particles towards the opposite electrode so that they were collected in the cyclone beneath the opposite electrode at each value of electric field intensity was also calculated; this value is called the critical charge. Hence, it was then possible to associate a particle charge variation, Δq, with each electric field variation, ΔE, relative to the mass fraction, ΔW.

As a consequence, the test methodology enabled the determination of the charge distribution on ash and carbon particles for each test sample. By comparing the charge distribution on W-ash and WD-ash, and by comparing the carbon–ash separation efficiency of freshly collected ash with that of W-ash and WD-ash, it was possible to determine the effect of surface moisture removal and the residual effect of long-term weathering.

3. Results and discussion

Table 1 shows the results obtained by the procedure described above. The critical charge values needed to move the charged particles toward the opposite electrode and above the flow splitter at the bottom of the electric field zone for each value of applied voltage were also calculated by solving the equation of motion of charged particles in the gas flow field under the influence of the applied electric field [9]. By associating with each field variation ΔE the particle charge variation from $q-\Delta q$ to q, it was possible to estimate the mass of particles ΔW with sufficient charge to be attracted by the opposite electrode. Further information on this approach are presented in Appendix A. These calculations gave a critical charge for mineral ash particles of 0.0012 pC at an applied voltage of 12 kV: all particles not moved at this voltage were considered to have a charge less than 0.0012 pC and were considered not to be charged or to be *poorly charged*. In the same way, the critical charge for mineral ash particles at an applied voltage of 3 kV was 0.005 pC. These calculations also gave a critical charge for carbon particles of 0.061 pC at an applied voltage of 12 kV: all carbon particles not moved at this voltage were considered to have a charge less than 0.061 pC and were considered not to be charged or to be poorly charged. In the same way, the critical charge for carbon particles at an applied voltage of 3 kV was 0.25 pC. In Table 2 the critical charges for either ash and carbon particles at different voltages are presented.

Furthermore, as we measured the particle mass ΔW (ash and carbon fractions) collected by the cyclones at each field variation, it was possible to derive a direct association between del ΔQ and ΔW, i.e. the distribution of particle charge over the mass of ash and carbon particles.

Fig. 2 plots the charge distributions for ash and carbon particles of the W-ash sample. The overall average charge of the mineral ash particles was near zero but the particles were more positively charged than shown in published results [2,6]. Furthermore, the ash

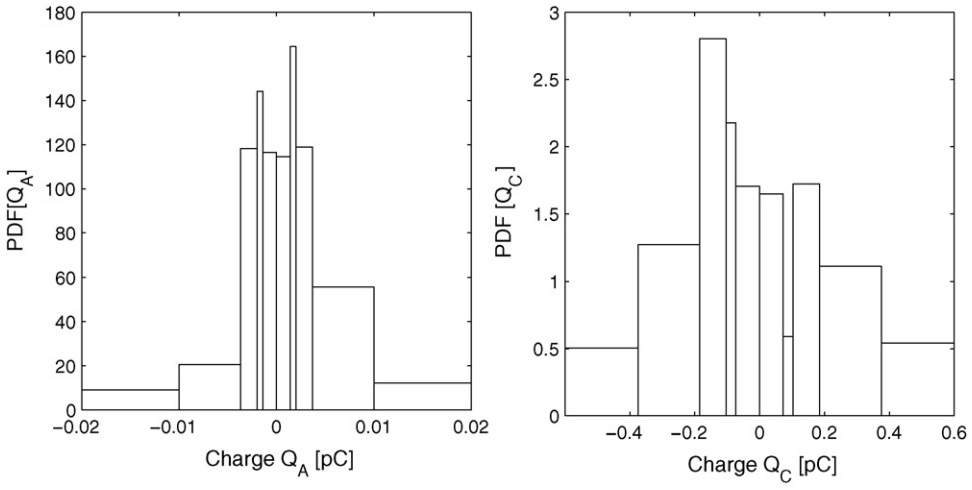

Fig. 2. Charge distribution for mineral fraction (Q_A) and unburned carbon (Q_C) of W-ash.

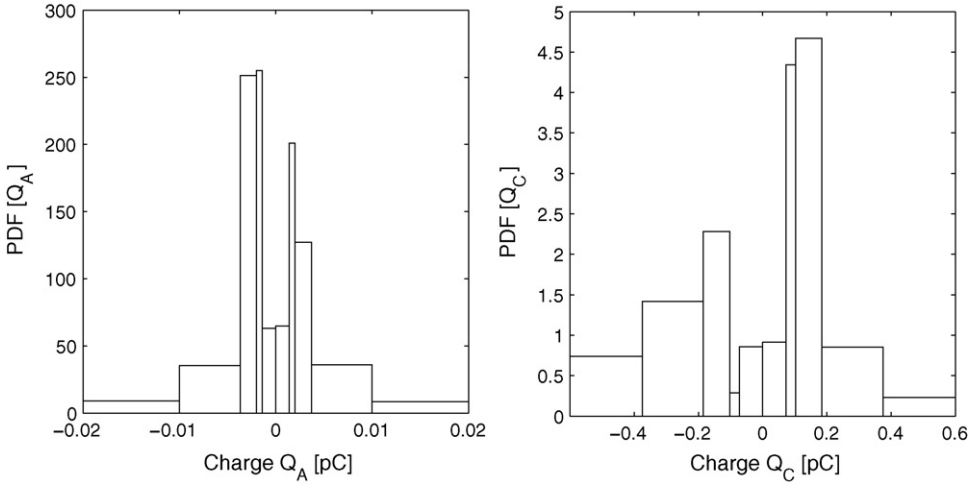

Fig. 3. Charge distribution for mineral fraction (Q_A) and unburned carbon (Q_C) of WD-ash.

particles were weakly charged, with most values below 0.005 pC regardless the polarity; the number of negatively charged particles was less than the number of positively charged particles. On the other hand, carbon particles displayed a peak in the charge distribution at slightly negative values with most of the particle mass characterized by negative polarity. This polarity is opposite of the behaviour expected for combustion fly ash. Thereby, it is clear that weathering creates surface modifications that cause particle polarities opposite of what so far have been exploited for triboelectrostatic beneficiation.

The charge distributions of mineral ash and carbon particles in weathered-then-dried sample were also determined using the procedure described above (Fig. 3). The overall, greatest change caused by drying was a reduction in the mass fraction of uncharged or neutral particles for both carbon and mineral ash species.

Fig. 4 summarizes the results obtained at the highest voltage (12 kV) for W-ash and WD-ash samples: for clarity, particle charge was divided into three classes, i.e. negative, positive and neutral, with the critical charge for mineral ash and carbon particles at 12 kV establishing the mass fraction values. As suggested by comparing the charge distributions, drying resulted in a decrease from 15 to 3% of the neutral fraction of ash particles, with an equal increase in positive and negative fractions. As for carbon fraction, neutral particles decreased from 15 to 5% as a result of drying, and the neutral particles all became positive after moisture removal.

Unfortunately, the extent of this charge reversal for the WD-ash was not sufficient to achieve efficient carbon–ash separation in comparison to that for the freshly collected (FC) ash even in an RP configuration (see Fig. 5). The reader is referred to citation [8] for explanation of how Yield and LOI_{dec} were calculated. One reason for the WD-ash to exhibit poor carbon–ash separation is expected to be the result of its wide distribution of particle charge that encompasses both positive and negative values for carbon and ash particles. Even a reduction in the number of neutral particles for the WD-ash did not result in a significant enhancement in overall separation performance. The bipolarity and magnitude of surface charge established during tribocharging was significantly compromised on W-ash and WD-ash and practically eliminated carbon–ash separation in comparison to the FC-ash.

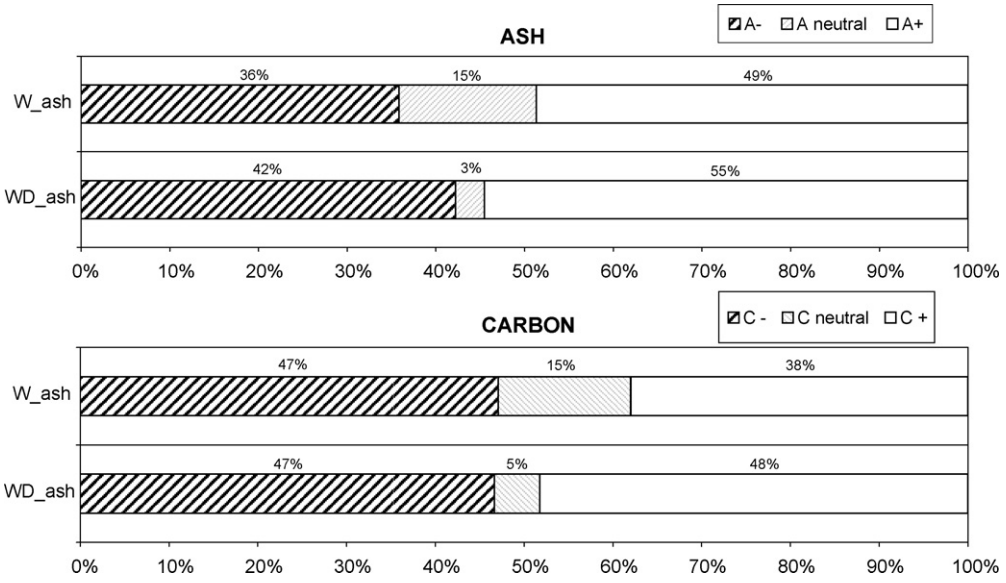

Fig. 4. Comparison between negative, neutral, positive mass of weathered and weathered-then-dried samples.

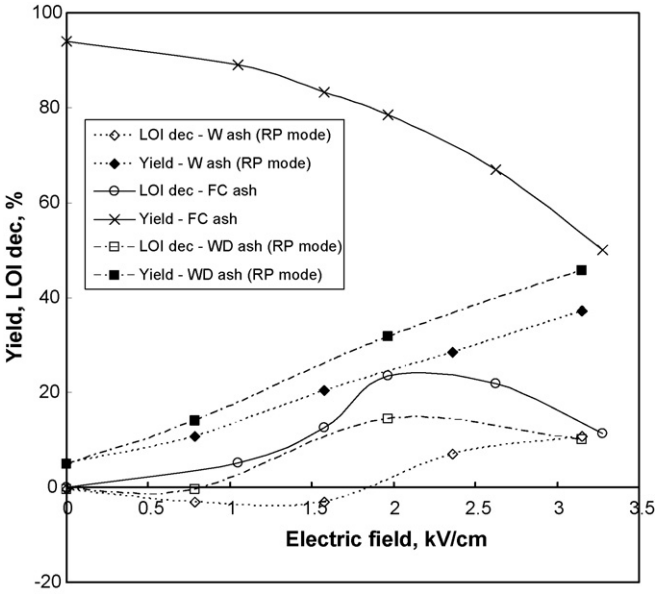

Fig. 5. Comparison between Yield and LOI decrease of FC, W and WD-ash.

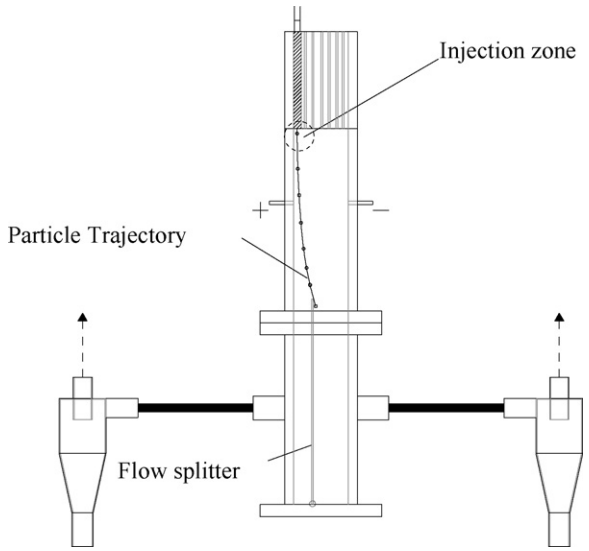

Fig. A.1. Schematic of particle deflection in the separation chamber under the influence of the electric field.

4. Conclusions

The purpose of this study was to analyze the effect of fly ash weathering, i.e. exposure to atmospheric conditions for an extended period, on carbon–ash separability and concomitant particle charge and polarities. A new protocol was developed that allowed charge distributions to be measured along with product masses during triboelectrostatic testing. For the Italian ash studied (LOI~30%) weathering created particle surfaces that under tribocharging conditions attained polarities opposite of that normally seen and overall low charge values. Although the charge distributions measured for the weathered-then-dried ash were more alike that expected from freshly collected ashes, the changes caused by removing surface moisture did not result in significant improvements is carbon–ash separability. It is evident that other surface modifications occurred during weathering, like surface oxidation, alkaline oxide carbonation, or enhanced surface concentrations of soluble ions, that were not reversible by heating. Nevertheless, the charge measurement protocol developed when coupled with triboelectrostatic test results such as mass yields and LOI analyses gave an overall improved approach for providing fundamental insight that could lead to better triboelectrostatic beneficiation performances.

Acknowledgments

The financial support for the present study by Regione Puglia under grant 220/06 “Progetto T.R.I.Ce.” POR Puglia 2000–2006 is gratefully acknowledged.

Appendix A

A.1. Derivation of ash and carbon critical charge

Evidently not all the particles entering the separator have the same charge as it depends on parameters attaining the tribocharging in the pneumatic line. For example, it has been found experimentally and theoretically that the probability density function (PDF) of particle charge for silica beads follows a Gumbel distribution [10].

As for a particle mixture (ash and unburned carbon) it is not possible either to predict nor directly measure the particle charge distribution.

Nevertheless, it is possible to indirectly derive the correspondence between a certain mass fraction ΔW to the charge q characterizing that fraction, e.g. the particle charge distribution.

The critical charge of a particle (ash or carbon) has been defined as the minimal charge that a particle must have under a certain electric field in the separator to be deflected from the injection zone toward the opposite electrode (see Fig. A.1).

The calculation of the particle trajectories in the separator was carried out using computational fluid dynamics, as detailed elsewhere [9]. In this appendix the techniques and main steps undertaken to perform such calculations are outlined.

A.1.1. Gas flow field

A commercial CFD code (CFX) was used to calculate the gas flow field and particles trajectories in the separator. The separation chamber was discretized in one million of elements with an unstructured mesh and the Navier–Stokes equations with a standard $k-\varepsilon$ model of turbulence were solved for the airflow distribution. The three-dimensional turbulent flow field was calculated in a computational domain with the size of 37.5 mm × 50 mm × 350 mm consisting of the separation chamber. A hybrid unstructured mesh of different elements (from 500,000 up to 1,500,000) is used in this study. Mass and momentum balance equations are integrated over the elements of the unstructured mesh. The standard model $k-\varepsilon$ was employed to simulate the turbulent motion with a sufficient accuracy and low CPU time cost. The following assumptions for the model were taken: (1) the fluid is incompressible, (2) the turbulent flow field is isotropic, and (3) the boundary conditions of smooth wall and no slip were chosen. The two-phase flow enters the separator at 7 m/s through a slit 3 mm wide thus creating a plane jet. A honeycomb structure at the inlet of the separation chamber allows the air at atmospheric pressure to be sucked into the cell were a slight negative pressure is set by means of a vacuum pump. The simulations of the flow field were carried out investigating a range of velocity at the cyclones outlet ranging between 1.4 and 35 m/s.

A.1.2. Particle motion in the separator

Particle tracking inside the separation chamber allows trajectories of the charged particles to be followed from the diffuser to the cyclones outlet. The assumption of dilute flow was made during the simulation, so that influence of particle motion on gas flow and particle–particle collisions were neglected: the particle tracking routine employed was than based on the hypothesis of one-way coupling between gas and particles [11,12]. Particles are injected in the separator with the same velocities as local airflow and with several angles φ from the direction of the z-axis. We assumed that φ is expressed by a normal distribution with average $\varphi_{av} = 0$ and standard deviation σ_φ. The following steps could be undertaken to carry out the simulation of particle motion in the electric field generated by the parallel plate electrodes inside the separator:

1. Solve the electric field neglecting the space charge ρ_E created by the charged particles using Laplace equation with the proper boundary conditions.
2. Calculate the charged particle trajectories with the Lagrangian approach considering aerodynamic and electrical forces acting on the particles:

$$m_p \frac{dv_p}{dt} = \frac{1}{8}\pi\rho d^2 C_D |v_f - v_p|(v_f - v_p) + \frac{\pi d^3 \rho_f}{6}\frac{dv_f}{dt} + \frac{1}{6}\pi d^3(\rho_p - \rho_f)g + F_E \quad (1)$$

   where v_p and v_f are the particle and fluid velocity, respectively, C_D is the drag coefficient [5] and F_E is the electric force q_E, q being the particle charge and E the electric field;
3. Calculate the space charge distribution ρ_E inside the separator.
4. Solve the electric filed by using the Poisson equation with the space charge obtained from the previous step.
5. Repeat steps 2–4 until solution is convergent.

This numerical technique was originally proposed by Elmoursi and Castle [13]. In our case only steps 1–3 were considered as the space charge was considered sufficiently small to not affect the electric field distribution.

References

[1] R. Gupta, D. Gidaspow, T. Wasan, Electrostatic separation of powder mixtures based on the work functions of its constituents, Powder Technology 75 (1993) 79–87.
[2] H. Ban, T.X. Li, J.C. Hower, J.L. Schaefer, J.M. Stencel, Triboelectrostatic separation of unburned carbon from fly ash. Preprint, division of fuel chemistry, American Chemical Society 41 (1996) 609–613.
[3] A. Iuga, L. Calin, V. Neamtu, A. Mihalcioiu, L. Dascalescu, Tribocharging of plastics granulates in a fluidized bed device, Journal of Electrostatics 63 (2005) 937–942.
[4] G. Dodbiba, J. Sadaki, K. Okaya, A. Shibayama, T. Fujita, The use of air tabling and triboelectric separation for separating a mixture of three plastics, Minerals Engineering 18 (2005) 1350–1360.
[5] J.D. Bittner, S.A. Gasiorowski, STI's 6 Years of Commercial Experiences in Electrostatic Beneficiation of Fly Ash. International Ash Utilization Symposium, CD Version, 2001, 9 pp.
[6] H. Ban, T.X. Li, J.C. Hower, J.L. Schaefer, J.M. Stencel, Dry triboelectrostatic beneficiation of fly ash, Fuel 76 (8) (1997) 801–805.
[7] J. Baltrus, J. Diehl, Y. Soong, W. Sands, Triboelectrostatic separation of fly ash and charge reversal, Fuel 81 (2002) 757–762.
[8] F. Cangialosi, M. Notarnicola, L. Liberti, P. Caramuscio, G. Belz, T. Gurupira, J.M. Stencel, Significance of surface moisture removal on triboelectrostatic beneficiation of fly ash, Fuel 85 (2006) 2286–2293.
[9] F. Cangialosi, F. Crapulli, G. Intini, L. Liberti, M. Notarnicola, Modelling of triboelectrostatic separation for industrial by-products, WIT Transactions on Ecology and the Environment 92 (2006) 95–104.
[10] F. Cangialosi, L. Liberti, M. Notarnicola, J.M. Stencel, Monte-Carlo simulation of pneumatic tribo-charging in two-phase flow for high-inertia particles, Powder Technology 165 (2006) 39–51.
[11] L.J.S. Bradbury, J. Riley, The spread of a turbolent plane jet issuing into a parallel moving air stream, Journal of Fluid Mechanics 27 (1967) 381–394.
[12] G. Gousbet, A. Berlemont, Eulerian and Lagrangian approaches for predicting the behaviour of discrete particles in turbulent flows, Progress in Energy and Combustion Science 25 (1998) 133–159.
[13] A.A. Elmoursi, G.S.P. Castle, Modelling of corona characteristics in a wire-duct precipitator using the charge simulation technique, IEEE Transactions on Industry Applications 23 (1987) 95–102.